

Revealing the Electron–Phonon Coupling in a Conjugated Polymer by Single-Molecule Spectroscopy**

By Richard Hildner, Ulrich Lemmer, Ullrich Scherf, Marin van Heel, and Jürgen Köhler*

In recent years π -conjugated polymers have attracted considerable attention because features such as fast and efficient energy-transfer, nonlinear optical behavior, and chemical modification of their spectral characteristics make conjugated polymers promising candidates for the design and development of novel optoelectronic devices with tailored properties, such as organic light-emitting diodes, organic photovoltaic cells, and “plastic” lasers.^[1–4] Their electronic and optical properties are determined to a large extent by the electron–phonon coupling strength, which is a measure for the rigidity of the polymer backbone upon electronic excitation or injection of charge carriers into the polymer chain.^[1,5–7] This key parameter strongly influences the efficiency of charge- and energy-transfer processes in conjugated polymers,^[5–7] and is therefore of great practical interest for possible applications. However, the pronounced structural disorder, which is an inherent feature in this type of functional materials,^[1,8–10] as well as strong spectral diffusion processes of the optical transitions^[11,12] have prevented a direct determination of this parameter thus far. Here, we employ single-molecule spectroscopy in combination with pattern recognition techniques, which allows us to retrieve the profile of the electronic spectrum and concomitantly the electron–phonon coupling strength in a methyl-substituted ladder-type poly(*para*-phenylene) (MeLPPP, see inset Fig. 1). The results indicate a weak electron–phonon coupling at low temperatures, consis-

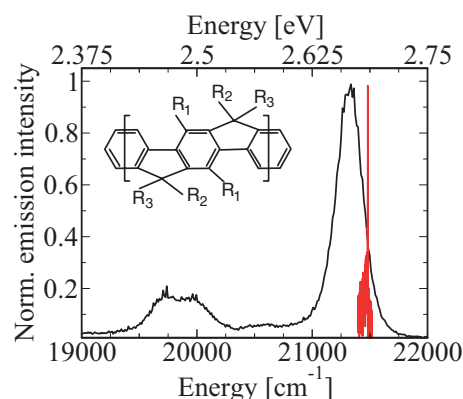


Figure 1. Emission spectra of a MeLPPP film and an individual MeLPPP chain. The emission spectrum of the thin MeLPPP-film is shown as the black curve, and the emission spectrum of the purely electronic 0–0 transition of an individual MeLPPP-chain embedded in *n*-hexadecane as the red curve. Both spectra have been recorded at 1.5 K and have been normalized for better comparison. The chemical structure of MeLPPP is also shown (R_1 : *n*-hexyl; R_2 : 1,4-decylphenyl; R_3 : methyl).

tent with the fast excitation energy transfer processes that have been observed for this polymer.^[13]

Conjugated polymers are organic macromolecules that consist of tens to hundreds of covalently bound molecular building blocks that are arranged in a chainlike structure. Their photophysical properties are governed by an extended π -electron system that determines the character of the lowest electronically excited states.^[5,6,8,9] However, owing to conformational disorder, kinks, and coiling of the polymer chain as well as the presence of chemical impurities the electronic excitations are not delocalized along the entire polymer backbone. At present the widely accepted picture is that a conjugated polymer can be considered as a chain of segments, each comprising typically 5–10 chemical repeat units. The electronic excitation energy is localized within a segment, which is commonly referred to as chromophore or site, and transferred efficiently between these segments by hopping processes.^[1,5,8,9] As a consequence of this, the emission stems only from very few chromophores on a chain. Experimental evidence for this model has been obtained mainly from site-selective fluorescence spectroscopy.^[1,9]

Whereas it is consensus that the electronic properties are determined to a large extent by the conformation of the polymer chain,^[8,10] the prediction of these properties for a random chain conformation in a disordered matrix is difficult; however, prediction of such properties is of key importance for

[*] Prof. J. Köhler, R. Hildner
Experimentalphysik IV and BIMF
Universität Bayreuth
Universitätsstrasse 30, 95447 Bayreuth (Germany)
E-mail: juergen.koehler@uni-bayreuth.de
Prof. U. Lemmer
Lichttechnisches Institut
Universität Karlsruhe (TH)
Kaiserstrasse 12, 76131 Karlsruhe (Germany)
Prof. U. Scherf
Fachbereich C – Mathematik und Naturwissenschaften &
Institut für Polymertechnologie
Universität Wuppertal
Gauss-Strasse 20, 42097 Wuppertal (Germany)
Prof. M. van Heel
Department of Biological Sciences
Imperial College London
London SW7 2AY (UK)

[**] We thank Ralf Schmidt from Image Science (Berlin) for his help with the IMAGIC software. This work was financially supported by the German Research Foundation (DFG), which is gratefully acknowledged.

the design of novel polymers for optoelectronic devices. Hence, it would be of crucial interest to obtain detailed information about the relevant parameters that describe the electronic structure of the excited states, that is, the spread in the site energy of individual chromophores, the interaction strength between the chromophores, and, in particular, the strength of the electron–phonon interaction.

Typically, the purely electronic (0–0) transition of an organic molecule embedded in a matrix gives rise to a homogeneously broadened zero-phonon line (ZPL) accompanied by a relatively broad phonon-side band (PSB).^[14] The ZPL results from the purely electronic transition, and the PSB from an electronic transition and the simultaneous excitation of vibrational modes (phonons) in the local environment of the emitting chromophore. The intensity ratio between the ZPL and the PSB, that is, the profile of the electronic spectrum, is determined by the electron–phonon coupling strength. A measure for the electron–phonon coupling strength is provided by the Debye–Waller factor $a = I_{\text{ZPL}} / (I_{\text{ZPL}} + I_{\text{PSB}})$, where I_{ZPL} (I_{PSB}) is the integrated intensity of the ZPL (PSB), respectively.

The great difficulty in determining the various parameters that play a role for the description of the electronic structure of conjugated polymers is the fact that the optical ensemble spectra are inhomogeneously broadened as a result of the large heterogeneity in the polymer samples.^[1,8–10] Therefore, conventional optical spectroscopy, which averages over large ensembles, provides only limited information about the properties of the electronically excited states. To avoid this complication, single-molecule techniques have been employed by several groups.^[10–12,15–21] This has led to the observation of a drastically reduced inhomogeneous line width of the 0–0 emission, and has allowed to obtain detailed information about excitation energy transfer pathways,^[11,15,16] chain conformations,^[10–12,17,18] the coherence length of electronic excitations,^[19] and photon antibunching from single polymer chains.^[20,21] However, any variation in the local environment of the emitting chromophore leads to changes of the local interactions and, concomitantly, to fluctuations of the electronic levels. In the optical spectra these fluctuations appear as spectral shifts of the optical transition on various time scales (spectral diffusion). As a consequence of this, even for single polymers, the PSB can not be retrieved because of temporal averaging during data acquisition.

To reveal the electron–phonon coupling strength in conjugated polymers we employed low-temperature single-molecule fluorescence spectroscopy on MeLPPP-chains in combination with a multivariate statistical pattern recognition algorithm^[22,23] for data analysis. This allowed us to resolve the spectral profile of the 0–0 emission and to determine the electron–phonon coupling strength in MeLPPP directly despite strong spectral diffusion processes and noisy single-molecule spectra.

In Figure 1 we overlaid the emission spectra from a MeLPPP film (black) and an individual polymer chain embedded in *n*-hexadecane (HD, red), both recorded at 1.5 K.

The ensemble spectrum features a purely electronic transition at $21\,300\text{ cm}^{-1}$ accompanied by a vibronic progression at $19\,850\text{ cm}^{-1}$. The 0–0 transition is inhomogeneously broadened (full width at half maximum (FWHM) 230 cm^{-1}), which reflects the intrinsic structural and energetic disorder in the ensemble of conjugated polymers. As evidenced by the spectrum of the individual polymer this line width can be reduced by several orders of magnitude, here to 2.6 cm^{-1} (FWHM, corresponding to $325\text{ }\mu\text{eV}$), by avoiding ensemble averaging.

For a detailed study of the spectral profile of the 0–0 transition we successively recorded several hundreds of emission spectra from an individual chromophore with an integration time of 1 s. Examples are shown in Figure 2, where stacks of 1000 consecutively acquired fluorescence spectra of a single MeLPPP-chain embedded in either HD (Fig. 2a, top) or polystyrene (PS, Fig. 2c, top) are displayed. The 0–0 transitions of individual chromophores can be identified in each single spectrum, and their “spectral trails” can be followed throughout the stacks of spectra. Typically, such an individual spectrum is extremely noisy and does not allow for a quantitative analysis of the profile of the electronic transition. The averages of all 1000 individual spectra are shown at the bottom of Figure 2a and c. The spectra feature relatively broad and structureless bands with line widths of 75 cm^{-1} (FWHM) for MeLPPP in HD and 38 cm^{-1} for MeLPPP in PS. These findings are in agreement with recent results obtained by others.^[11,16] Apparently, the main contribution to the line width of the time-averaged spectra stems from spectral diffusion processes reflecting fluctuations in the local environment of the emitting site.^[11,12] We exclude the option that emission from different sites on the same polymer chain contributes to the spectral fluctuations, because those were not accompanied by changes of the orientation of the transition dipole moment (data not shown).

As a consequence of the spectral fluctuations, neither the individually recorded spectra within a stack nor the time-averaged spectra permit a quantitative analysis of the spectral profile of the electronic transition. To overcome these limitations we applied a multivariate statistical pattern recognition algorithm (MSA) which has been demonstrated to be a valuable tool to retrieve the profiles of electronic spectra from individual objects in disordered systems.^[24] Briefly, in the MSA analysis each individual spectrum in a stack of spectra (e.g., Fig. 2a, top) is interpreted as a 1D image. By pattern recognition these spectra are grouped into a predetermined number of classes (here typically 5–10) according to their statistical similarity, such that the variance between the classes is maximized and the total intra-class variance is minimized (in a mathematical, least-squares sense). From this procedure we obtain the class-averaged spectra (CAS), that is, the average of only those individual spectra that have been assigned to a particular class. In simple words, the algorithm ensures that only those individual spectra are averaged that are “sufficiently similar”. Further details about this algorithm can be found elsewhere.^[22,23] The achievement of this approach is that contributions to the line width from spectral diffusion processes, occurring on time scales slower than the integration

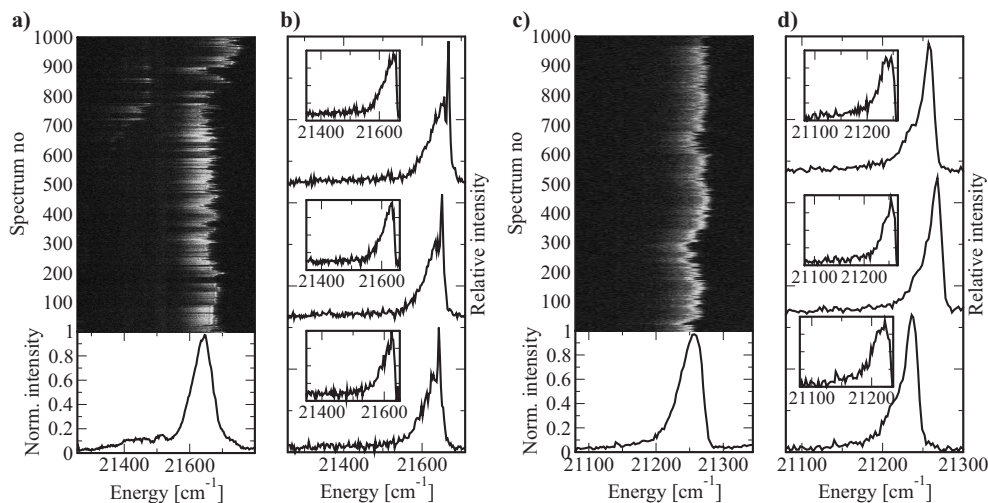


Figure 2. Single-molecule emission spectra from MeLPPP embedded in HD and PS, and the results of the statistical analysis. a,c) 2D representations of 1000 fluorescence spectra of the 0–0 transitions of individual MeLPPP-chains embedded in HD and PS, respectively. The individual spectra have been recorded consecutively with an integration time of 1 s at a temperature of 1.5 K. The horizontal axis corresponds to energy, the vertical axis to the spectrum number or, equivalently, to time, and the emission intensity is given by the grey scale. The corresponding total averages of all 1000 spectra are depicted at the bottom of each pattern and feature line widths (FWHM) of 75 cm⁻¹ (MeLPPP in HD) and 38 cm⁻¹ (MeLPPP in PS). b,d) Three examples of normalized class-averaged spectra obtained by the application of the multivariate statistical algorithm to the stacks of fluorescence spectra. The insets show an expanded view of the phonon side bands after subtraction of a Lorentzian fitted to the high-energy tail of the zero-phonon lines.

time for the individual spectra (here: 1 s) are eliminated. Hence, the spectra from an individual chromophore can be registered with a drastically reduced spectral line width without the usual trade-off between spectral and/or temporal resolution versus signal-to-noise ratio.

For the stacks of fluorescence spectra presented in Figure 2 (a and c, top) three examples of the corresponding CAS are shown in Figure 2b and d, respectively. The spectral profiles of the CAS show a sharp line and a shoulder in the low-energy wing. Accordingly, we assign the narrow feature to the ZPL and the broad feature in the low-energy tail of the ZPL to the PSB of the transition. For MeLPPP in HD (PS) the line widths of the ZPLs were distributed between 2.6 and 38 cm⁻¹ (7 and 45 cm⁻¹), and both distributions peak at 12 cm⁻¹. For a quantitative analysis of the spectral profile of the CAS a Lorentzian was fitted to the high-energy tail of the ZPL and then subtracted from the CAS to uncover the remaining PSB, as shown in the insets of Figure 2b and d. From these data we determined the mean phonon energy ω_m , which is the center energy of the PSB with respect to the center energy of the ZPL, and the Debye–Waller factor a .

The distributions of the Debye–Waller factor a both for MeLPPP in HD and MeLPPP in PS are depicted in Figure 3. Irrespective of the host, the distributions feature a peak at about 0.5 and cover a range from 0.25–0.9 which is, in general, indicative of weak electron–phonon coupling. The obvious question that arises concerns the origin of the low-frequency vibrations that are coupled to the electronic transition. Do they correspond to nuclear motions of the host matrix, or do they reflect phonon modes of the polymer backbone as suggested in earlier work?^[11]

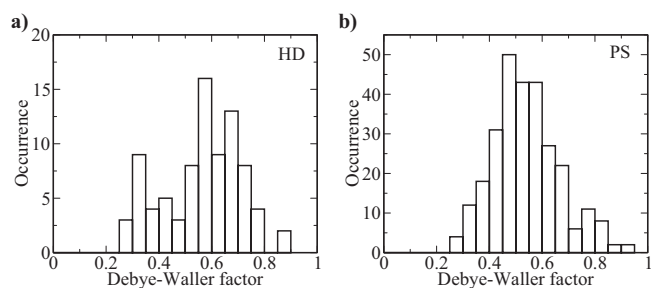


Figure 3. Histograms of the Debye–Waller factor a . a) The distribution for single MeLPPP chains embedded in a HD host, and b) the distribution for MeLPPP chains embedded in a PS matrix.

To answer this question we analyzed the distributions of the mean phonon energies in more detail. For MeLPPP in HD we find a bimodal distribution with maxima at 15 cm⁻¹ and 40 cm⁻¹, whereas for MeLPPP in PS this distribution is centered at 30 cm⁻¹ and appears broader compared with the distribution for MeLPPP in HD. In contrast with the distributions of the Debye–Waller factors, those of the mean phonon energies are clearly different for the two host materials. Insight into the nature of the phonon modes of the matrix materials has been obtained from inelastic neutron scattering.^[25–27] To facilitate comparisons with the results from those experiments, we divided the distributions of the mean phonon energies by ω_m^2 for the presentation in Figure 4.

For HD, unfortunately, neutron scattering experiments at 25 K did not allow for the detection of vibrational modes with energies below 20 cm⁻¹, and only a vibrational mode at about 37 cm⁻¹ could be detected.^[25] However, such experiments on

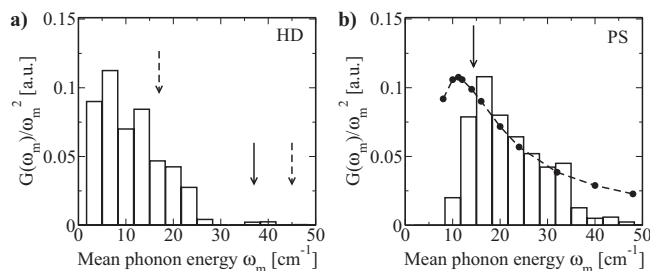


Figure 4. Distributions of the mean phonon energy ω_m . For better comparison with literature data the distributions have been divided by ω_m^2 ; $G(\omega_m)$ denotes the density of phonon states. a) Distribution of ω_m for single MeLPPP chains embedded in HD (bars). The arrows indicate the energetic positions of low-frequency modes that have been obtained by inelastic neutron scattering on *n*-alkanes at 25 K: the full arrow marks the energetic position of a low-energy mode at 37 cm^{-1} in an HD sample^[25] and the broken arrows indicate two low-energy modes at 17 and 45 cm^{-1} in *n*-octadecane.^[25] b) Distribution of ω_m for single MeLPPP chains in PS (bars). The filled circles reproduce the boson peak of PS, which has been obtained by inelastic neutron scattering at 80 K [27]. The arrow marks the peak position (14.4 cm^{-1}) of the boson peak measured by inelastic neutron scattering on PS at 10 K [26].

n-octadecane (OD), an *n*-alkane that is slightly longer than HD, revealed two modes with energies of 17 cm^{-1} and 45 cm^{-1} at 25 K, which were assigned to intramolecular modes of the alkane chain.^[25] The frequencies of the modes obtained by neutron scattering are indicated in Figure 4a by the full arrow for HD and by the broken arrows for OD. Taking into account the different length of OD with respect to HD, which is reflected by the frequency shift of the mode at higher energy from 45 cm^{-1} to 37 cm^{-1} , the phonon frequencies found by neutron scattering are in very good agreement with the mean phonon frequencies obtained by our single-molecule experiments.

For amorphous materials, such as PS, a universal feature that can be observed in neutron scattering as well as Raman spectroscopy is the so-called Boson peak at energies in the range of 10–70 cm^{-1} . This peak corresponds to a maximum in the ratio $G(\omega)/\omega^2$, where $G(\omega)$ denotes the density of phonon states and ω the phonon frequency. Its microscopic origin was suggested to be due to the presence of interacting quasi-localized low-frequency modes in amorphous materials.^[28] In Figure 4b we compare the distribution of mean phonon energies derived from our experiments on individual MeLPPP chains in PS (bars) with the Boson peak of PS as obtained by inelastic neutron scattering experiments at 80 K (filled circles^[27]). We note that the two data sets are superimposed without adjusting any parameters. The arrow in Figure 4b marks the position of the maximum of the Boson peak obtained for PS at 10 K^[26] which is closer to our experimental conditions. As evidenced by Figure 4b the data from the two independent experimental approaches, that is, neutron scattering and single-molecule spectroscopy, are in good quantitative agreement.

These comparisons both for MeLPPP in HD and MeLPPP in PS provide strong evidence that the phonons giving rise to the PSB in the optical spectra of individual MeLPPP chains

correspond to low-energy vibrational modes of the host matrix rather than intramolecular modes of MeLPPP and its side groups. However, we cannot fully rule out that low-frequency vibrational modes of MeLPPP contribute to the observed PSBs as well. Quantum-chemical calculations for ladder-type *para*-phenylene oligomers yielded an intramolecular longitudinal acoustic mode with significant electron-phonon coupling strength.^[29,30] The energy of this mode varied between 60–160 cm^{-1} , depending on the oligomer length and the computational method.^[29,30] However, even for the unlikely case that the observed PSBs reflect exclusively the coupling with intramolecular vibrations of MeLPPP our data allow us to conclude that the electron-phonon coupling strength in MeLPPP is weak. An important consequence of this statement is that the structural reorganization of the polymer backbone upon electronic excitation is small. Hence, the Stokes shift between absorption and emission is small as well and the strong spectral overlap between donor and acceptor chromophores on the polymer chain enhances the rates for excitation energy transfer along the MeLPPP chain.^[6,7] This is consistent with fast energy migration processes that have been recently detected for the same polymer system by time-resolved spectroscopy.^[13]

In conclusion, we were able to retrieve the profile of the electronic spectra of individual MeLPPP-chains by combining low-temperature single-molecule spectroscopy with multivariate statistical pattern recognition techniques for data analysis. We found values of about 0.5 for the Debye–Waller factor for MeLPPP embedded in both HD and PS, which indicates only weak electron-phonon coupling irrespective of the matrix material. Additionally, we found strong evidence that the low-frequency phonon modes, which are coupled to the electronic transitions, stem from vibrations of the host matrix, suggesting an even weaker intrachain electron-phonon coupling in MeLPPP. This observation is of crucial importance for the development of theoretical models that describe the electronic and optical properties of these functional materials. Our single-molecule data yield information that is not accessible by conventional ensemble spectroscopy and might stimulate further theoretical studies to describe the optoelectronic properties of this fascinating class of materials.

Experimental

The single-molecule samples were prepared by dissolving the conjugated polymer MeLPPP in toluene at typical concentrations of 20 nm. This solution was further diluted in HD or a PS–toluene solution (HD/PS–toluene:MeLPPP–toluene 100:1). A drop of the diluted solution was sandwiched between a quartz substrate and a quartz cover slip (MeLPPP in HD) or spin-coated onto a quartz substrate (MeLPPP in PS), mounted in a home-built cryostat, and cooled to 1.5 K. To perform fluorescence spectroscopy the MeLPPP chains were excited by a frequency-doubled titanium:sapphire laser (Tsunami, Spectra-Physics; frequency doubler: Model 3980, Spectra-Physics) operating at 430 nm with a repetition rate of 81 MHz and a pulse width of 1.5 ps (FWHM) through a home-built microscope that could be operated in either confocal or widefield mode. The objective of the

microscope had a numerical aperture of 0.85 (Microthek) and allowed a lateral resolution of about 350 nm at $\lambda = 430$ nm when immersed in liquid helium. The fluorescence was passed through a set of dielectric filters, spectrally dispersed in a spectrograph (SpectraPro-150, Acton Research Corporation, 600 lines mm^{-1} or 250 IS, Bruker, 1800 lines mm^{-1}) and imaged onto a sensitive charge-coupled device (CCD) camera (SensiCam QE, PCO). The spectral resolution was 3.5 cm^{-1} (SpectraPro-150) and 0.8 cm^{-1} (250 IS), respectively. The selection of individual MeLPPP-chains took place as follows. First, we acquired a widefield image of a $20 \mu\text{m} \times 20 \mu\text{m}$ region of the sample and chose a well-isolated chain. Subsequently, we switched the microscope to the confocal mode and moved the focus of the objective by means of a telecentric lens system, in such a manner that the excitation volume and the position of the individual polymer chain coincided.

Received: November 28, 2006

Revised: February 13, 2007

Published online: June 26, 2007

-
- [1] M. Pope, C. E. Swenberg, *Electronic Processes in Organic Crystals and Polymers*, Oxford University Press, Oxford **1999**.
- [2] R. H. Friend, R. W. Gymer, A. B. Holmes, J. H. Burroughes, R. N. Marks, C. Taliani, D. D. C. Bradley, D. A. dos Santos, J. L. Brédas, M. Logdlund, W. R. Salaneck, *Nature* **1999**, 397, 121.
- [3] F. Hide, M. A. Diaz-Garcia, B. J. Schwartz, A. J. Heeger, *Acc. Chem. Res.* **1997**, 30, 430.
- [4] U. Scherf, S. Riechel, U. Lemmer, R. F. Mahrt, *Curr. Opin. Solid State Mater. Sci.* **2001**, 5, 143.
- [5] W. Barford, *Electronic and Optical Properties of Conjugated Polymers*, Clarendon Press, Oxford **2005**.
- [6] J. L. Brédas, D. Beljonne, V. Coropceanu, J. Cornil, *Chem. Rev.* **2004**, 104, 4971.
- [7] V. May, O. Kühn, *Charge and Energy Transfer Dynamics in Molecular Systems*, Wiley-VCH, Berlin **2000**.
- [8] B. J. Schwartz, *Annu. Rev. Phys. Chem.* **2003**, 54, 141.
- [9] H. Bässler, B. Schweitzer, *Acc. Chem. Res.* **1999**, 32, 173.
- [10] D. Hu, J. Yu, K. Wong, B. Bagchi, P. J. Rossky, P. F. Barbara, *Nature* **2000**, 405, 1030.
- [11] F. Schindler, J. M. Lupton, J. Feldmann, U. Scherf, *Proc. Natl. Acad. Sci. USA.* **2004**, 101, 14 695.
- [12] T. Pullerits, O. Mirzov, I. G. Scheblykin, *J. Phys. Chem. B* **2005**, 109, 19099.
- [13] R. Hildner, U. Lemmer, U. Scherf, J. Köhler, *Chem. Phys. Lett.* **2006**, 429, 103.
- [14] K. K. Rebane, *Impurity Spectra of Solids*, Plenum, New York, **1970**.
- [15] D. A. Vanden Bout, W. Yip, D. Hu, D. Fu, T. M. Swager, P. F. Barbara, *Science* **1997**, 277, 1074.
- [16] J. G. Müller, U. Lemmer, G. Raschke, M. Anni, U. Scherf, J. M. Lupton, J. Feldmann, *Phys. Rev. Lett.* **2003**, 91, 267403.
- [17] T. Huser, M. Yan, L. J. Rothberg, *Proc. Natl. Acad. Sci. USA* **2000**, 97, 11187.
- [18] J. D. White, J. H. Hsu, W. S. Fann, S. Yang, G. Y. Pern, S. A. Chen, *Chem. Phys. Lett.* **2001**, 338, 263.
- [19] F. Dubin, R. Melet, T. Barisien, R. Grousson, L. Legrand, M. Schott, V. Voliotis, *Nat. Phys.* **2006**, 2, 32.
- [20] C. W. Hollars, S. M. Lane, T. Huser, *Chem. Phys. Lett.* **2003**, 370, 393.
- [21] P. Kumar, T. Lee, A. Mehta, B. G. Sumpter, R. M. Dickson, M. D. Barnes, *J. Am. Chem. Soc.* **2004**, 126, 3376.
- [22] L. Borland, M. van Heel, *J. Opt. Soc. Am. A* **1990**, 7, 601.
- [23] M. van Heel, B. Gowen, R. Matadeen, E. V. Orlova, R. Finn, T. Pape, D. Cohen, H. Stark, R. Schmidt, M. Schatz, A. Patwardhan, *Quart. Rev. Biophys.* **2000**, 33, 307.
- [24] C. Hofmann, H. Michel, M. van Heel, J. Köhler, *Phys. Rev. Lett.* **2005**, 94, 195501.
- [25] D. A. Braden, S. F. Parker, J. Tomkinson, B. S. Hudson, *J. Chem. Phys.* **1999**, 111, 429.
- [26] K. Inoue, T. Kanaya, S. Ikeda, K. Kaji, K. Shibata, M. Misawa, Y. Kiyonagi, *J. Chem. Phys.* **1991**, 95, 5332.
- [27] R. Inoue, T. Kanaya, K. Nishida, I. Tsukushi, K. Shibata, *Phys. Rev. Lett.* **2005**, 95, 056102.
- [28] M. A. Ramos, U. Buchenau, in *Tunneling Systems in Amorphous and Crystalline Solids* (Ed: P. Esquinazi), Springer, Berlin **1998**, Ch. 9.
- [29] H. Wiesenhofer, E. Zojer, E. J. W. List, U. Scherf, J. L. Brédas, D. Beljonne, *Adv. Mater.* **2006**, 18, 310.
- [30] S. Karabunarliev, E. R. Bittner, M. Baumgarten, *J. Chem. Phys.* **2001**, 114, 5863.
-